The following supplement accompanies the article

Heat budget responses of the eastern China seas to global warming in a coupled atmosphere–ocean model

Di Tian, Jian Su*, Feng Zhou, Bernhard Mayer, Dmitry Sein, Han Zhang, Daji Huang, Thomas Pohlmann

*Corresponding author: jis@dmi.dk

Climate Research 79: 109–126 (2019)

Supplement: Model validation

Conducting a hindcast simulation using re-analysis data is a common method to validate the model performance, since available observational data can be used for the validation. The three hindcast simulations based on the ERA-Interim dataset are as follows: (1) H-EARI, which has the same computational grid and coupling time step as the 20C. (2) H-EARI-L40, same as H-ERAI, but the REMO has 40 hybrid vertical levels. (3) H-EARI-R25, same as H-ERAI, but the horizontal resolution is about 25 km for the REMO model and the coupling time step is 1 hour.

The spatial distributions of annual mean SST forced by different atmospheric data sets (H-ERAI, H-ERAI-L40, H-ERAI-R25 and 20C) for the hindcast simulations are compared with annual mean SST data derived from the OISST and WOA13 datasets (Fig. A1). The model succeeds in reproducing the spatial pattern of the ECSs' SST, with lower SST occurring in the northern ECSs and higher SST in the southern ECSs. In addition, the MPIOM model can also reproduce the spatial pattern of surface current over the ECSs region, when forced by the four above-mentioned meteorological data sets (Fig. A2), although the simulated Kuroshio Current is somewhat stronger than indicated datasets from AVISO and OSCAR. The results with all four forcing data sets are similar. This close similarity also holds true for the surface heat fluxes, when MPIOM simulations are forced by H-ERAI, H-ERAI-L40 and H-ERAI-R25 (Fig. A3 and A4). This close similarity of results for different meteorological forcing data sets suggests that in the frame of the current study a multi-member ensemble approach was not essential to improve the reliability of the simulations.

The multi-annual means of the lateral volume transport in the runs H-ERAI, H-EARI-L40 and H-EARI-R25 also show that the TAS and SBS are two main passages for water intrusion from the open ocean into ECSs, while the TUS is an important export pathway (Table A1). Comparing these hindcast runs forced by ERA-Interim with result of the 20C run forced by the MPI-ESM output, their magnitudes of the volume transports crossing each section are in same order (Table A1 and Table 1). Moreover, no obvious differences are found among these three ensemble members with different atmospheric forcing, since the differences between each of these two members are smaller than their respective standard deviations. The same is true for the air-sea heat exchange over the ECSs (Table A2). By means of this sensitivity and validation exercise, we can infer that the REMO/MPIOM model produces consistent results and with our model setting a multi-ensemble approach is not necessary to perform a reasonable scenario projection.

Table S1 Multi-annual means and standard deviations of volume transports crossing OLBs under three cases forced by ERA-Interim dataset. The OLBs are indicated as red dots in Figure 1. Positive transport is directed inward. Unit: Sv (1 Sv=10^6 m^3 s^{-1}).

Fence name	H-ERAI (1980–2012)	H-ERAI-L40 (1980–2012)	H-ERAI-R25 (1980–2012)
SBS	0.54±0.26	0.49±0.26	0.62±0.23
TAS	1.78±0.14	1.82±0.11	1.71±0.12
TUS	–2.32±0.19	–2.30±0.20	–2.32±0.17
Net	0.01±0.01	0.01±0.02	0.01±0.01

Table S2 Multi-annual means and standard deviations of surface heat flux into the ECSs under three cases forced by ERA-Interim dataset. Positive transport is directed inward. Unit: W m^{-2}.

Components	20C (1970-2005)	H-ERAI (1980-2012)	H-ERAI-L40 (1980-2012)	H-ERAI-R25 (1980-2012)
Shortwave radiation	151.56±3.81	144.24±3.07	144.65±3.30	145.58±3.71
Longwave radiation	–53.23±1.89	–51.21±1.74	–51.59±1.93	–52.40±1.78
Latent heat flux	–100.90±4.79	–104.27±4.9	–107.33±5.33	–103.91±5.17
Sensible heat flux	–25.70±2.45	–25.97±2.80	–26.64±2.90	–25.93±2.86
Net_SF	–28.27±6.48	–37.22±7.68	–40.92±7.79	–36.66±7.70

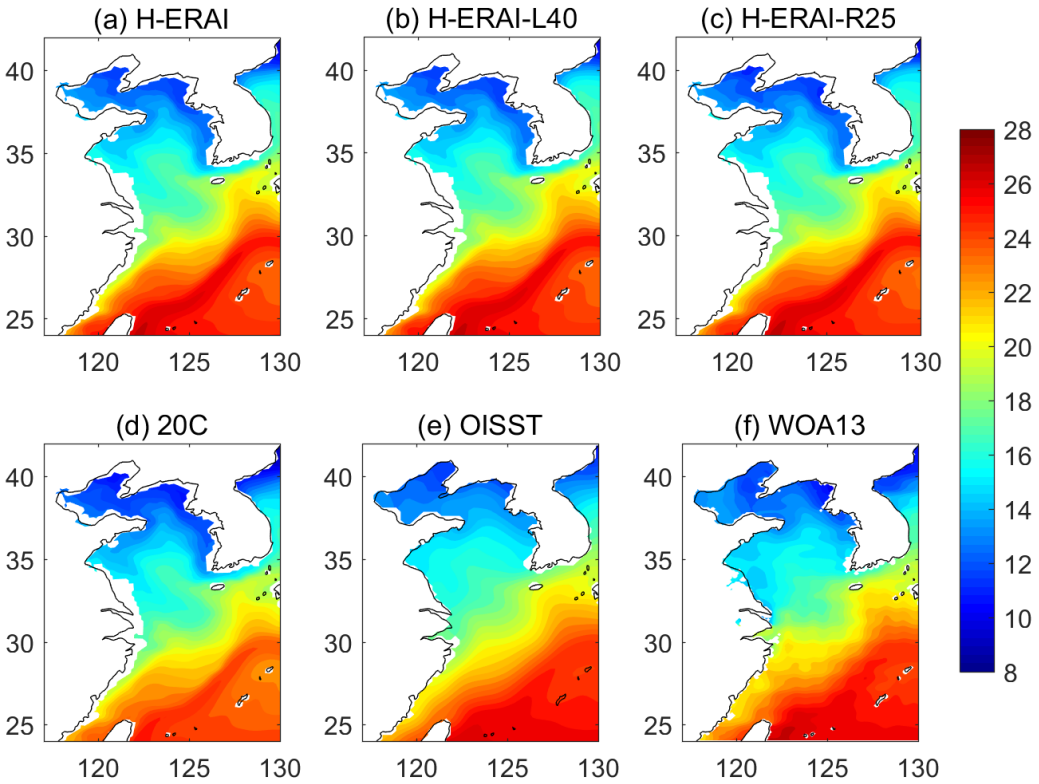

Figure S1. Multi-annual mean sea surface temperature (℃) over the ECSs for the (a) H-ERAI, (b) H-ERAI-L40, (c) H-ERAI-R25, (d) 20C, (e) OISST and (f) WOA13. (a–e) are averaged from 1982 to 2005.

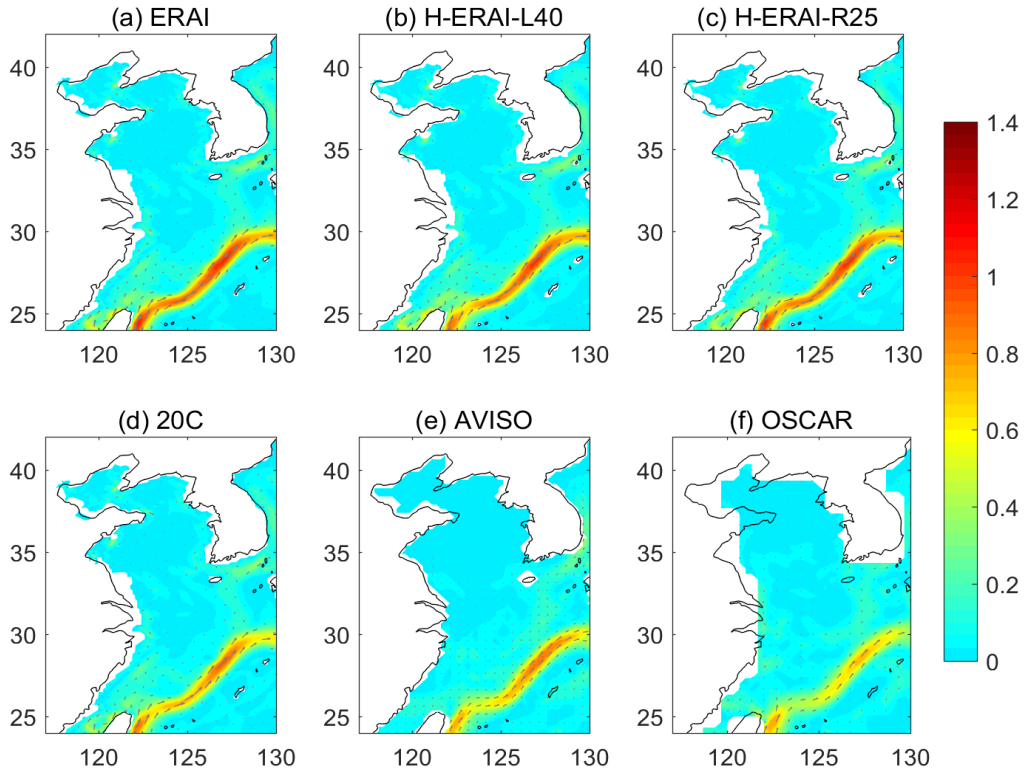

Figure S2. Multi-annual mean sea surface velocity (m s^{-1}) over the ECSs for the (a) H-ERAI, (b) H-ERAI-L40, (c) H-ERAI-R25, (d) 20C, (e) AVISO and (f) OSCAR, averaged from 1993 to 2005.

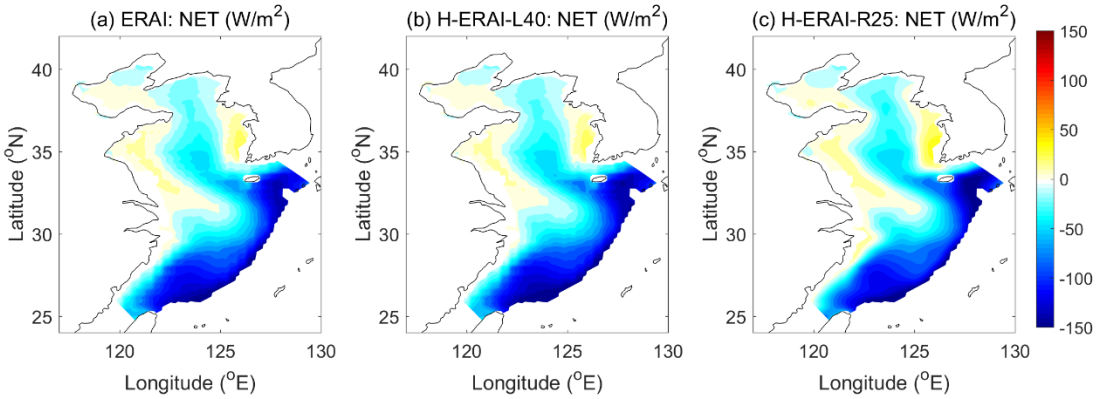

Figure S3. Multi-annual mean surface net heat flux over the ECSs for the (a) H-ERAI, (b) H-ERAI-L40 and (c) H-ERAI-R25, averaged from 1980 to 2012.

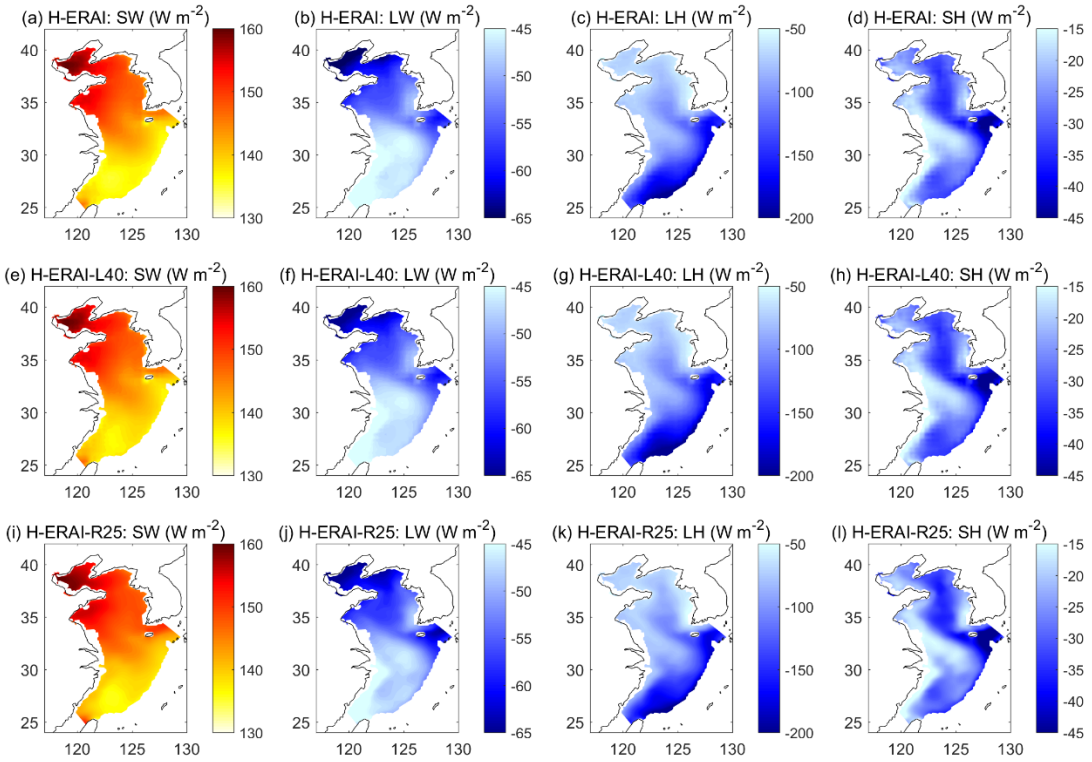

Figure S4. Multi-annual mean surface heat flux over the ECSs for the (a–d) H-ERAI, (e–h) H-ERAI-L40 and (i–l) H-ERAI-R25, averaged from 1980 to 2012. From left to right: shortwave radiation, longwave radiation, latent heat flux, and sensible heat flux.